

## Superdeformed bands in $^{191}\text{Tl}$

S. Pilotte,\* C.-H Yu,<sup>†</sup> H. Q. Jin,<sup>‡</sup> J. M. Lewis, and L. L. Riedinger  
*Department of Physics, University of Tennessee, Knoxville, Tennessee 37996*

Y. Liang, R. V. F. Janssens, M. P. Carpenter, T. L. Khoo, T. Lauritsen, and F. Soramel<sup>§</sup>  
*Argonne National Laboratory, Argonne, Illinois 60439*

I. G. Bearden  
*Purdue University, West Lafayette, Indiana 47907*

C. Baktash, J. D. Garrett, N. R. Johnson, I. Y. Lee,<sup>||</sup> and F. K. McGowan  
*Oak Ridge National Laboratory, Oak Ridge, Tennessee 37830*

(Received 13 April 1993)

High spin states in the  $^{191}\text{Tl}$  nucleus have been populated via the  $^{159}\text{Tb}(^{36}\text{S},4n)$  reaction at 165 MeV. Two weakly populated rotational bands have been observed with properties (energy spacings and dynamic moments of inertia) very similar to those of other superdeformed bands in the  $A \sim 190$  region. The two bands can be interpreted as signature partners which exhibit some signature splitting for rotational frequencies  $\hbar\omega \geq 0.2$  MeV. They are interpreted within the framework of cranked Woods-Saxon calculations as being based on the proton  $i_{13/2}(\Omega=5/2)$  intruder orbital, in agreement with pairs of superdeformed bands seen in neighboring odd Tl nuclei.

PACS number(s): 21.10.Re, 23.20.En, 23.20.Lv, 27.80.+w

### I. INTRODUCTION

High spin states in nuclei with mass  $A \sim 190$  have been the subject of much interest since the discovery of superdeformation in  $^{191}\text{Hg}$  [1]. The region has been extensively explored recently, both theoretically and experimentally. In excess of 30 superdeformed (SD) bands have now been reported in this mass region [2] and many aspects of the data have been interpreted with some success in cranked Woods-Saxon calculations with pairing (see [2–6], for example). The nucleus  $^{192}\text{Hg}$  plays a central role in this context as it is often regarded as a doubly magic SD nucleus. Large shell gaps are calculated [3,7] to occur in the single-particle spectrum for  $Z = 80$  and  $N = 112$  at a quadrupole deformation  $\beta_2 \sim 0.5$ . A single SD band has been reported in this nucleus [5,8,9].

Within the framework of the cranked Woods-Saxon calculations mentioned above, the SD bands in the neighboring nuclei can be understood in terms of particles or holes coupled to the  $^{192}\text{Hg}$  core. For example, neutron excitations built on the  $j_{15/2}$  high- $N$  intruder orbital [10] as well as on other orbitals close to the Fermi surface in

the SD well have been identified in the  $^{189-194}\text{Hg}$  nuclei [2]. The role of the  $i_{13/2}$  proton intruder has been discussed in connection with SD bands in the Tl isotopes. Furthermore, the various SD bands have also been shown to relate closely to the  $^{192}\text{Hg}$  SD band [11], as striking similarities in transition energies between bands in different nuclei have been noticed [11,12] (so-called “identical” bands).

In the present paper, we report on the discovery of two SD bands in  $^{191}\text{Tl}$ , a nucleus with two neutron “holes” and one proton “particle” outside the  $N = 112$ ,  $Z = 80$  core. This is the lightest Tl nucleus in which superdeformation has been observed. Thus far, two SD bands have been reported in each of the odd-even isotopes  $^{193,195}\text{Tl}$  [13,14], while six SD bands have been observed in both of the odd-odd  $^{192,194}\text{Tl}$  [6,12] nuclei. The similarities between the two SD bands observed in this work and those seen in  $^{193}\text{Tl}$  and  $^{195}\text{Tl}$  are emphasized, and an interpretation in terms of a specific proton excitation is presented.

The experimental techniques used in this study are described in Sec. II. The main results are presented in Sec. III. The interpretation of the data is given in Sec. IV, which is followed by a brief conclusion.

### II. EXPERIMENTAL TECHNIQUES

High spin states in  $^{191}\text{Tl}$  have been populated with the  $^{159}\text{Tb}(^{36}\text{S},4n)$  reaction at 165 MeV. This particular reaction was chosen because it produces the residual  $^{191}\text{Tl}$  nuclei under conditions of excitation energy ( $E^* \sim 24$  MeV) and angular momentum ( $\ell_{\text{max}} \sim 45\hbar$ ) which are very similar to those used to populate SD bands successfully in nuclei throughout this mass region. In a first mea-

\*Present address: Department of Physics, University of Ottawa, Ottawa, Canada, K1N-6N5.

<sup>†</sup>Present address: Department of Physics, University of Rochester, Rochester, NY 14627.

<sup>‡</sup>Present address: Department of Physics, Rutgers University, New Brunswick, NJ 08903.

<sup>§</sup>Permanent address: Padova University, I 35131, Padova, Italy.

<sup>||</sup>Present address: Lawrence Berkeley Laboratory, Berkeley, CA 94720.

surement, a beam from the Holifield Heavy Ion Research Facility at Oak Ridge National Laboratory was used. In a second experiment, a beam of the same energy was provided by the ATLAS superconducting linear accelerator at Argonne National Laboratory. The same target was used in both experiments and consisted of a stack of two self-supporting  $500 \mu\text{g}/\text{cm}^2$  thick foils. At Oak Ridge, coincidence  $\gamma$ -ray events were collected with the Spin Spectrometer comprising 19 Compton-suppressed Ge detectors and 52 NaI(Tl) scintillators. Each valid event was defined by the requirement that a minimum of two suppressed Ge detectors fire in coincidence with a minimum of six NaI(Tl) counters. Approximately  $200 \times 10^6$  events were collected in this way on magnetic tape. In the Argonne experiment, coincidence events were collected with the 12 Compton-suppressed Ge detectors surrounding the inner array of 50 hexagonal BGO elements which constitute the Argonne-Notre Dame BGO  $\gamma$ -ray facility. In this measurement four array detectors were required to fire in prompt coincidence with a minimum of two suppressed Ge detectors. Approximately  $120 \times 10^6$  events were written to tape.

In the analysis of the two data sets, symmetrized, Doppler-shift corrected  $E_{\gamma_1} - E_{\gamma_2}$  matrices were constructed after proper correction of the data for random and pile-up events. In these matrices, long rotational cascades were enhanced by requiring that a large number of NaI(Tl) ( $K \geq 10$  or 12) or BGO detectors ( $K \geq 8$  or 10) fire in coincidence with the event. This selection also enhances the relative yield of transitions in the  $4n$  reaction channel over that of  $\gamma$  rays in the competing  $5n$  channel leading to  $^{190}\text{Tl}$ . As a result, a minimum of 60% of the events in the coincidence matrices under analysis belonged to  $^{191}\text{Tl}$ . In the case of the Argonne data, matrices were also generated according to the angle of the detectors with respect to the beam direction. In the Argonne Notre Dame BGO  $\gamma$ -ray facility the detectors are located at  $34.5^\circ$ ,  $90^\circ$ , and  $146.5^\circ$ , and information on the multipolarity of the transitions can be derived from the measurement of DCO (Directional Correlations from Oriented Nuclei) ratios. The definition and a discussion of the use of these ratios for the experimental arrangement of interest can be found in Ref. [15].

### III. RESULTS

The detailed analysis of the coincidence matrices revealed the presence of two bands with average energy differences between consecutive transitions of 37.1 and 36.5 keV, respectively. These differences are very similar to those seen in SD bands in this region and are consistent with the spacing expected for a SD shape [7]. Furthermore, as in most of the SD bands near  $A = 190$  [2], the energy spacings between consecutive transitions in the two bands vary in a smooth and systematic way from  $\sim 40$  keV at the bottom of the bands to  $\sim 33$  keV at the highest  $\gamma$ -ray energies. Spectra for the two bands are presented in Fig. 1. As can be seen in the figure, band 1 is characterized by 9 (possibly 10) transitions. The number of transitions in band 2 is smaller, i.e., 7 (possibly 8)

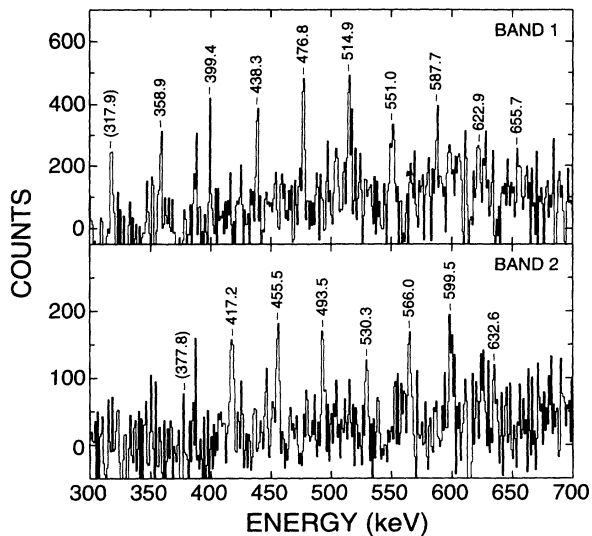


FIG. 1. Efficiency corrected  $\gamma$ -ray spectra for the two SD bands in  $^{191}\text{Tl}$ . These spectra were obtained by summing the cleanest coincidence gates (see text for detail). Transitions for which the placement is uncertain are given within parentheses. The  $\gamma$ -ray energies are uncertain to 0.3 keV for the strongest transitions and 0.6 keV for the higher energy, weaker  $\gamma$  rays.

$\gamma$  rays have been identified. The spectra in Fig. 1 are the sum of the cleanest coincidence gates (438, 515, and 551 keV for band 1 and 417, 493, and 529 keV for band 2). The two bands presented in Fig. 1 have very weak intensity and most of the transitions are contaminated with other lines of greater intensity. As a result, the spectra presented in the figure contain some contaminants. Nevertheless, for most of the transitions the expected coincidence relationships between band members were verified from the inspection of individual gates as well as from the observation of grid patterns in the two dimensional coincidence matrix. The transitions for which an assignment to one of the bands is less certain are given in parenthesis.

The placement of the two bands in  $^{191}\text{Tl}$  is based on the observation of the 387, 713, 748, and 753 keV transitions belonging to the  $9/2[505]$  proton yrast band in  $^{191}\text{Tl}$  [16] in coincidence with the lines of interest. However, because transitions in the two bands are extremely weak, it was impossible to delineate the feeding pattern into the yrast line with any accuracy, as the intensity of the  $\gamma$  rays of interest was found to be very sensitive to the way the background was subtracted in the coincidence spectra. We used the Palameta and Waddington method [17] in creating our final background subtracted matrix. The assignment to  $^{191}\text{Tl}$  was further strengthened by the measured sum-energy and multiplicity (fold) distributions in the NaI(Tl) or BGO arrays. Both quantities were found to peak at values only slightly higher than those measured for the  $^{191}\text{Tl}$  yrast transitions. This observation is common for SD bands [2,18] and is thought to reflect the fact that the SD states are fed from the higher partial waves of the angular momentum distribution of the compound nucleus.

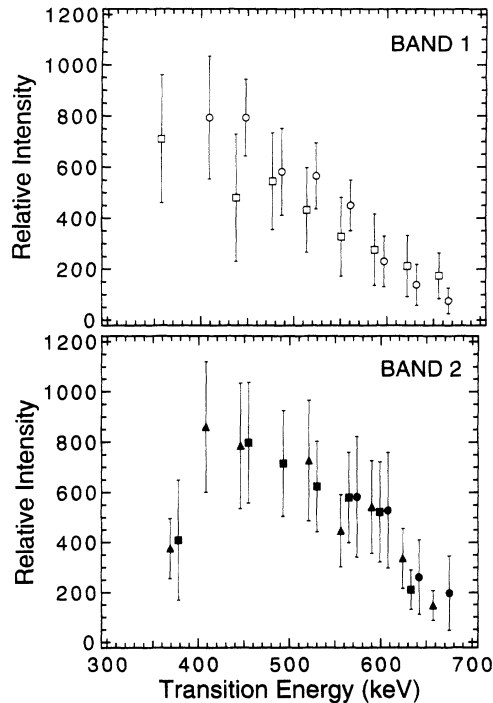


FIG. 2. Measured intensity distribution for the two SD bands in  $^{191}\text{Tl}$ . The individual intensities were obtained from coincidence spectra gated on the 358.7 (open circles), 399.4 (open squares), 417.2 (filled squares), 493.5 (filled triangles) and 566.0 (filled circles) keV SD transitions. Note that the data points corresponding to the 399.4, 493.5 and 566.0 keV gates have been shifted in energy by 9, -9, and 9 keV respectively to improve legibility.

Under the multiplicity condition outlined above, the total  $\gamma$ -ray flux through each band is about equal and represents at most 0.4% of the total  $^{191}\text{Tl}$  intensity. This flux is lower by at least a factor of 5 than the intensity measured in the SD bands of  $^{191}\text{--}^{194}\text{Hg}$  [1–3] for example. Figure 2 presents the intensity distributions along the two bands. These patterns are similar to those seen in all the SD bands of this region; i.e., the intensity decreases with increasing  $\gamma$ -ray energy for  $E_\gamma > 500$  keV. In the bottom part of the two cascades, the intensity seems to remain essentially constant over the lowest 3–4 transitions while the decay out towards the yrast states occurs as a sudden drain over 1–2 transitions. Transitions linking the two bands with the yrast states could not be found: No  $\gamma$ -ray with an intensity  $> 3\%$  of the 399 keV transition and an energy  $< 4.1$  MeV was observed in these data. Because of the low intensity and the fact that there are very few clean gates, multipolarity information could be obtained only for the strongest transitions in each band. The correlation data derived from the angle sorted matrices indicate that the transitions involved are of stretched  $E2$  character. In band 1, the DCO ratios were found to have values consistent with the expected value of 1.35 for the 399, 438, 476, 551, and 588 keV transitions. The same statement applies to the 417, 456, 494, 530, and 566 keV  $\gamma$  rays in band 2.

Finally, it should be mentioned that a thorough search

of the coincidence matrices for regular grid patterns with energy spacings corresponding to those expected for SD bands was also undertaken. The technique is very similar to that described in Ref. [19]. Besides the two SD bands reported above, no other signal could be found. It is estimated that any other SD band in  $^{191}\text{Tl}$  populated in the present experiment would have an upper intensity limit of less than 0.2% of all events in  $^{191}\text{Tl}$ .

From the description given above, it is clear that the two bands reported here have many properties similar to those observed in SD nuclei of the  $A \sim 190$  region. As a result, it is proposed that these two new bands correspond to the rotation of the  $^{191}\text{Tl}$  nucleus with very large prolate deformation and they are referred to as SD bands in the discussion hereafter.

#### IV. DISCUSSION

From a close inspection of Fig. 1, it can be seen that, for  $\gamma$ -ray energies smaller than  $\sim 500$  keV, the transition energies in one of the bands lie almost exactly midway between the energies of the transitions in the other band.

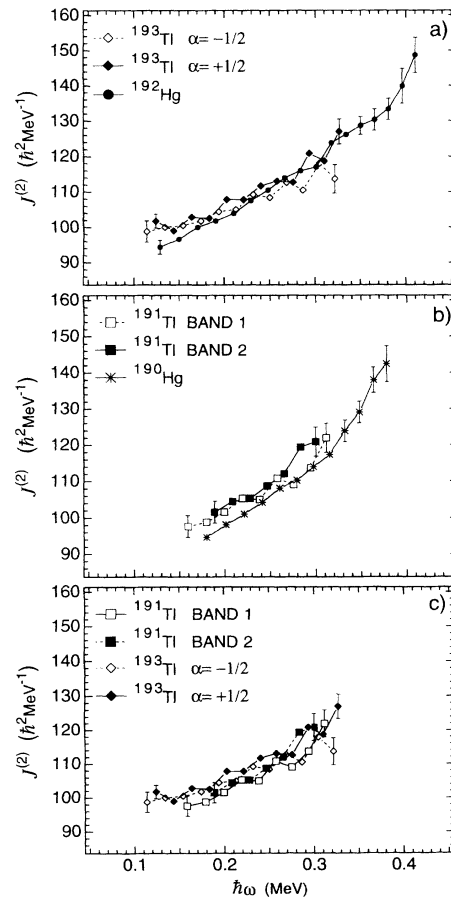


FIG. 3. Dynamic moments of inertia  $J^{(2)}$  in the nuclei  $^{191,193}\text{Tl}$  and  $^{190,192}\text{Hg}$  as a function of the rotational frequency  $\hbar\omega$ . Note that only the larger error bars are indicated. For most other points, the error bars are smaller and occasionally the size of the data point itself.

The situation is analogous to that observed previously in SD bands in the Tl isotopes [6,11–14] and in some of the Hg nuclei [2]. In analogy with the interpretation given in these various cases, we propose that bands 1 and 2 in  $^{191}\text{Tl}$  are signature partners exhibiting some degree of signature splitting at the highest rotational frequencies, as will be discussed below.

The evolution of the dynamic moment of inertia  $J^{(2)}$  as a function of the rotational frequency  $\hbar\omega$  for the two bands reported here is compared in Fig. 3 with that of previously established SD bands in  $^{193}\text{Tl}$  [13] and  $^{190,192}\text{Hg}$  [5,8,9,20]. From this figure several observations can be made. First, the moments of inertia are seen to rise with  $\hbar\omega$  for both bands in  $^{191}\text{Tl}$  as in the three other nuclei just mentioned. (In fact, the vast majority of the SD bands in the  $A \sim 190$  region exhibit such a smooth rise with  $\hbar\omega$  [2].) Secondly, the values of  $J^{(2)}$  are 1% to 3% smaller in  $^{191}\text{Tl}$  than in  $^{193}\text{Tl}$  for  $\hbar\omega$  between 0.2 MeV and 0.3 MeV [Fig. 3(c)], but the average rate of increase with  $\hbar\omega$  in the same range is larger in the lightest Tl isotope (14% in  $^{191}\text{Tl}$  vs 11% in  $^{193}\text{Tl}$ ). Finally, at the lowest frequencies, the value of  $J^{(2)}$  is larger than the corresponding value for the core SD nucleus  $^{190}\text{Hg}$  [Fig. 3(b)]. The rise in  $J^{(2)}$  over the entire frequency range is, however, larger in  $^{190}\text{Hg}$  than in the two bands of  $^{191}\text{Tl}$ : for  $0.2 < \hbar\omega < 0.3$  MeV, the rise is 17% in  $^{190}\text{Hg}$  and 14% in  $^{191}\text{Tl}$ . The situation is analogous to that reported in Ref. [13] where a similar comparison was made for  $^{193}\text{Tl}$  and its core SD nucleus  $^{192}\text{Hg}$ . The latter comparison is also presented in Fig. 3(a).

### A. Proposed configuration

Cranked shell model (CSM) calculations with pairing have been shown to reproduce a number of properties related to SD nuclei near  $A = 190$ , at least qualitatively [2–6,13]. For example, the smooth rise of  $J^{(2)}$  with  $\hbar\omega$  seen in most SD bands in this mass region has been attributed in the CSM calculations to the alignment under rotation of a pair of quasineutrons and/or quasiprotons occupying high- $N$  intruder orbitals ( $\nu j_{15/2}$  and/or  $\pi i_{13/2}$ ). Such an interpretation requires the presence of static neutron and proton pairing at the large deformations involved. The pairing is thought to be weaker in the SD well than near the groundstate, but detailed calculations of its precise characteristics (magnitude, dependence on  $\hbar\omega$  and spin, etc.) are currently lacking [2,5,20]. The most convincing experimental evidence for the presence of pairing in SD nuclei comes from so-called blocking measurements where the alignment of a pair of quasiparticles is blocked in odd-even or odd-odd nuclei by the presence of an odd quasiparticle in the orbital of interest (so-called Pauli blocking). Recently,  $J^{(2)}$  was found to be constant with  $\hbar\omega$  for two of the six SD bands of  $^{192}\text{Tl}$  [6], and this result was interpreted in terms of Pauli blocking of quasiparticle alignments in intruder orbitals.

CSM calculations with the Warsaw Woods-Saxon code [21] with parameters given in Ref. [22] have been performed in order to identify the possible configurations associated with the SD bands in  $^{191}\text{Tl}$ . The results are

very similar to those obtained earlier for  $^{193}\text{Tl}$  in Ref. [13], where the relevant single-particle energy diagrams and quasiparticle routhians can be found. The proton single-particle spectrum indicates the presence of a pronounced gap at  $Z = 80$  for  $\beta_2 \sim 0.5$ , and this gap remains open for all frequencies considered. Above this gap lies the third  $N = 6$  ( $i_{13/2}$ ) orbital with  $\Omega = 5/2$  ( $N$  is the principal quantum number of the state and  $\Omega$  denotes the angular momentum projection on the symmetry axis) which is located at least 500 keV lower in excitation energy than the next orbital. As in  $^{193}\text{Tl}$ , the most probable SD configuration would thus have the third  $i_{13/2}$  orbital occupied, and any excited proton SD configurations would likely involve the [514]9/2 or the [411]1/2 orbitals which are located above and below the Fermi surface, respectively. Adopting  $^{190}\text{Hg}$  as the SD core for  $^{191}\text{Tl}$ , the configuration associated with bands 1 and 2 in  $^{191}\text{Tl}$  can then be written as  $\pi 6_{5/2} \otimes ^{190}\text{Hg}$ , where the convention of labeling intruder orbitals as  $N_\Omega$  is used.

The fact that the odd quasiproton occupies an intruder orbital has at least two consequences for the evolution of  $J^{(2)}$  with  $\hbar\omega$ . First, the occupation of an additional  $\pi i_{13/2}$  orbital will result in an additional contribution to the dynamic moment of inertia with respect to the  $^{190}\text{Hg}$  core and, as seen experimentally [Fig. 3(b)], the  $J^{(2)}$  value for  $^{191}\text{Tl}$  is expected to be larger than that for  $^{190}\text{Hg}$  at the lowest rotational frequencies. Second, the rise of  $J^{(2)}$  with  $\hbar\omega$ , which in  $^{190}\text{Hg}$  is calculated to be due to the combined alignment of a  $i_{13/2}$  quasiproton and a  $j_{15/2}$  quasineutron pair [20,23], will only result from the alignment of the quasineutron pair in  $^{191}\text{Tl}$ , as the alignment of the quasiprotons is blocked by the occupation of the intruder orbital. Presumably, this feature accounts for the difference in the relative rise of  $J^{(2)}$  with  $\hbar\omega$  between  $^{191}\text{Tl}$  and  $^{190}\text{Hg}$  noted above. The CSM calculations also indicate that the SD well is characterized by a slightly smaller ( $\sim 5\%$ ) quadrupole deformation in  $^{191}\text{Tl}$  than in  $^{193}\text{Tl}$ . This feature reflects a small difference in deformation for the different even-even Hg core nuclei which has been discussed in Ref. [23,24]. The interaction strength between the crossing quasineutron configurations (responsible for the rise in  $J^{(2)}$ ) is also predicted to be somewhat larger at lower mass. Both of these effects will result in a sharper rise of  $J^{(2)}$  with  $\hbar\omega$  and could explain the difference mentioned above between the  $J^{(2)}$  values for  $^{191}\text{Tl}$  and  $^{193}\text{Tl}$ , in the same way as they have been proposed to account for the differences between the behaviors of  $J^{(2)}$  in  $^{190}\text{Hg}$  and  $^{192}\text{Hg}$  [20,23].

### B. Signature splitting

As already discussed for the case of  $^{193}\text{Tl}$  in Ref. [13], the  $6_{5/2}$  orbital is calculated to exhibit signature splitting for  $\hbar\omega > 0.2$  MeV, although the magnitude of this splitting and the exact frequency at which it occurs depend on the details of the CSM calculations. It was also pointed out in Ref. [13] that the  $6_{5/2}$  orbital is the only orbital close to the Fermi surface to exhibit a behavior similar to that seen in the data. Indeed, the [514]9/2 orbital is calculated to show signature splitting only for

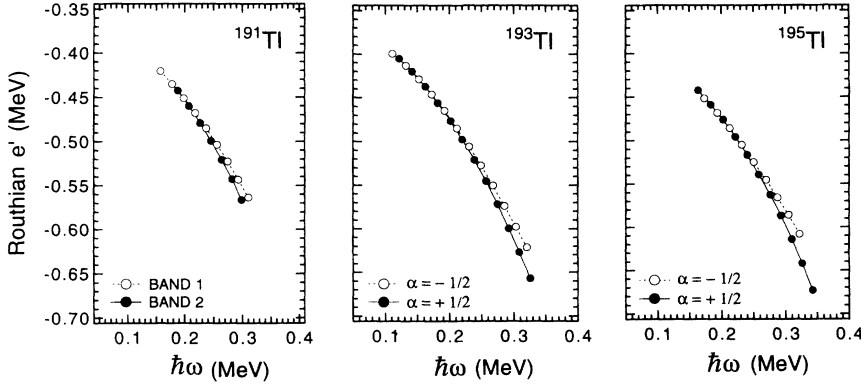


FIG. 4. Comparison between the experimental routians for the SD bands in the three odd Tl isotopes with  $A = 191, 193, 195$ . The parameters used to obtain the routians are discussed in the text.

$\hbar\omega > 0.4$  MeV, while splitting is present at all frequencies for the  $[411]1/2$  orbital. Within the framework of the CSM calculations it is likely that the SD bands seen in the three odd-even SD Tl nuclei ( $A = 191, 193, 195$ ) are associated with the same quasiproton configuration. Thus, it becomes interesting to compare the degree of signature splitting in all three cases in order to verify this assertion. Such a comparison is done in Fig. 4, where the experimental single-particle routians  $e'$  have been extracted for all three data sets. The computation of these routians requires knowledge of the excitation energies and spins involved in the bands as well as a phenomenological representation of the energy associated with the rotating nuclear core. Under the assumption that the bands are strongly coupled at low  $\hbar\omega$ , the excitation energies were arbitrarily taken as 1.13 MeV and 1.33 MeV for the two signatures, the rotating core was approximated using the Harris parametrization [25]  $E'_g(\omega) = -(\omega^2/2)J_0 - (\omega^4/4)J_1 + \hbar^2/(8J_0)$  with  $J_0 = 88 \hbar^2\text{MeV}^{-1}$  ( $^{191}\text{Tl}$ ) or  $J_0 = 90 \hbar^2\text{MeV}^{-1}$  ( $^{193,195}\text{Tl}$ ) and  $J_1 = 80 \hbar^4\text{MeV}^{-3}$ , and the spins were estimated with the method proposed in Ref. [8]. The small difference in the  $J_0$  value when going from the lighter Tl isotope to the two other is thought to reflect the slightly smaller deformation discussed above. We note that in all three nuclei, the spins derived in this way are half integers and differ by one spin unit from band 1 to band 2, as would be ex-

pected for strongly coupled bands in odd-even nuclei. As can be seen from Fig. 4, a comparable degree of signature splitting is apparent in all three odd-even SD nuclei. This conclusion is, however, dependent to some degree on the validity of the parameter set and the fitting procedure described above. This problem is circumvented in Fig. 5, where the energy shift  $\Delta E$  is plotted versus transition energy. The quantity  $\Delta E$  is defined as the difference between a transition energy in one band and the average of the two transitions closest in energy in the partner band; i.e.,

$$\Delta E = E_\gamma(I \rightarrow I - 2) - 1/2[E_\gamma(I + 1 \rightarrow I - 1) + E_\gamma(I - 1 \rightarrow I - 3)].$$

The energy shifts  $\Delta E$  in  $^{191}\text{Tl}$ ,  $^{193}\text{Tl}$ , and  $^{195}\text{Tl}$  are remarkably similar, both in their respective variation with transition energy and in their absolute magnitude. This observation supports the assignment of the same  $6_{5/2}$  configuration to the SD structures in the three SD nuclei and indicates that, for the three SD nuclei under discussion, the physical effects responsible for the rise of  $J^{(2)}$  and for the signature splitting are most likely of the same origin.

### C. Incremental alignment

One of the most surprising results to have come out of the superdeformation studies is the discovery, in neighboring nuclei, of SD bands with transition energies identical to within a few tenths of a keV. This feature was first reported for SD nuclei in the  $A \sim 150$  region [26], but has also been found to occur near  $A = 190$  [2,11,27]. Furthermore, recent investigations of nuclei at smaller deformations have also uncovered cases of bands with similar transition energies for nuclei in various regions of the periodic table [28–31]. For SD nuclei near  $A = 190$ , Stephens *et al.* [11,27] have proposed to compare all SD bands of the region to the “reference” SD band in  $^{192}\text{Hg}$  by studying the evolution with  $\hbar\omega$  of the incremental alignment  $\Delta i = 2\Delta E_\gamma/\Delta E_\gamma^r$ . In this expression  $\Delta E_\gamma$  is obtained by subtracting the transition energy in a band of interest from the closest transition energy in the reference SD band and  $\Delta E_\gamma^r$  is calculated as the energy difference between the two closest transitions in the SD band of the

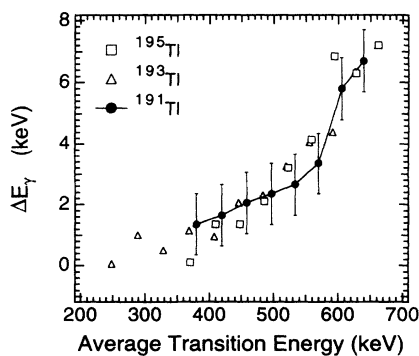


FIG. 5. Comparison between the energy shifts  $\Delta E$  in the two SD bands of the odd-even Tl isotopes (see text for details). The error bars are given for  $^{191}\text{Tl}$  only, but are representative of those found in the other cases.

reference. The SD  $^{192}\text{Hg}$  nucleus is chosen as the reference because of its presumed doubly magic character. It has been shown that, for many SD bands near  $A = 190$ ,  $\Delta i$  values cluster around values  $\Delta i = +1, 0$  for even-even nuclei and  $+0.5$  for odd-even nuclei [2,11,27]. This result is quite surprising as there is no a priori reason for such groupings, although it can be shown that these particular values of  $\Delta i$  are to be expected in the limit where the strong coupling model applies rigorously. The data for  $^{191}\text{Tl}$  do not fit in this systematics; i.e., when referred to  $^{192}\text{Hg}$ ,  $\Delta i$  decreases smoothly from  $-0.88$  to  $-1.22$  with  $\hbar\omega$  for band 1, while  $\Delta i$  decreases smoothly with  $\hbar\omega$  for band 2 from  $\Delta i = 0.2$  to  $\Delta i = 0$  before rising again to  $\Delta i = 0.2$  for the two highest frequency points. Thus, the two bands do not cluster around  $\Delta i = +0.5$  as would be expected for odd- $A$  nuclei. The situation is identical to that reported for  $^{193}\text{Tl}$  [13] and, as in this case, can be understood if the odd proton occupies the  $6_{5/2}$  orbital as proposed in Sec. IV A above, i.e., if  $^{191}\text{Tl}$  and  $^{192}\text{Hg}$  differ by the number of occupied intruder orbitals. Indeed, among all orbitals in the SD well, the intruder orbitals are those which vary the most in intrinsic energy with rotational frequency. Furthermore, quasiparticles in these orbitals tend to both change the deformation and align with rotation. As a result, these orbitals have the largest influence on the variations of  $J^{(2)}$  with  $\hbar\omega$  [2]. Attempts to choose  $^{190}\text{Hg}$  rather than  $^{192}\text{Hg}$  as the reference for  $^{191}\text{Tl}$  were found to be equally unsuccessful, presumably for the same reason.

#### D. Absolute SD intensity and decay out

It has been pointed out that both the absolute intensity with which SD bands are fed and the frequency at which the decay out of the SD bands towards the low lying yrast states occurs display a systematic trend in the Hg and Pb isotopes [23,32,33]. For example, while the absolute intensity with which the SD bands are fed in  $^{191}\text{Hg}$  and in the heavier isotopes is of the order of 2%, this quantity drops to 0.8% in  $^{190}\text{Hg}$  and  $< 0.5\%$  in  $^{189}\text{Hg}$ . This comparison between isotopes is particularly meaningful because in all cases the beam energy and the projectile-target combination have been optimized in order to study nuclei with similar initial excitation energy and angular momentum. The largest absolute intensity measured in the Tl isotopes is always smaller by at least a factor of 2 than that reported in the Hg isotone. Furthermore, a similar variation of the absolute intensity in the Tl isotopes can now also be seen. Indeed, the absolute intensity reported here for  $^{191}\text{Tl}$  (the isotone of  $^{190}\text{Hg}$ ) is lower than that reported for the heavier isotopes. Finally, the lowest transition energy in the SD bands of the Tl isotopes increases with decreasing mass in a similar way as do the SD bands reported in the Hg and Pb nuclei: This is illustrated in Fig. 6. For the purpose of comparison, we have adopted the convention proposed in Ref. [23,32] to define the transition of lowest energy in the SD band. This choice is of course arbitrary and only provides for consistency in mapping systematic changes in the global properties associated with the decay out.

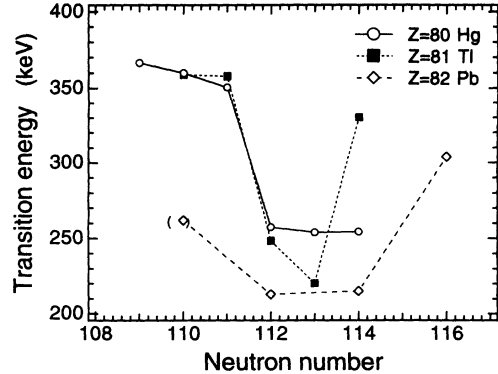


FIG. 6. Energy of the lowest SD transition (defined as the last low-energy  $\gamma$  ray carrying more than 50% of the SD intensity) in the yrast SD bands of the Hg, Tl and Pb isotopes.

The observed decrease of the SD intensity with decreasing mass number suggests that the lower limit of the SD region for the Tl isotopes occurs at neutron numbers similar to those at which it takes place for the Hg and Pb isotopes, i.e., in the vicinity of neutron number  $N = 108$ . This lower limit is in qualitative agreement with the results of cranked Strutinsky [7,24] and Hartree Fock [34] calculations indicating that the well depth of the SD minimum diminishes as one moves away from the  $N = 112$  closed SD shell toward lower values of  $N$ . It should, however, be pointed out that the decrease in SD population cannot be attributed to decrease in well depth alone, since the population intensity of a SD band is also related to the competition between the feeding of normal and SD states which is dependent on a number of factors of which the well depth is only one. The spin at which the depopulation of the SD bands occurs should be sensitive to the well depth as well. Even though the spins of the SD states have not been measured, there is evidence that  $\gamma$ -ray energies and spins are strongly correlated for SD bands [2,12,8,27]. For the Tl isotopes, the differences in spin implied by Fig. 6 could be as large as  $(4-6)\hbar$ . This large difference in spin contains physics information since several factors affect the decay out of the SD bands such as (i) the well depth and the barrier thickness, (ii) the excitation energy of the SD minimum, and (iii) the density of the normal states at the point of decay. As pointed out in Ref. [23,32], the trends shown in Fig. 6 for  $N < 112$  follow that of the calculated well depths and of the product of the well depths and the barrier thickness, while it is possible that the data points for  $N > 112$  reflect the increase of the excitation energy of the SD well. Clearly, a more firm conclusion about which parameters are the most important for the properties discussed here will have to wait for more detailed measurements.

#### V. CONCLUSION

Two SD bands have been observed in the present study of  $^{191}\text{Tl}$  with the  $^{159}\text{Tb}(^{36}\text{S},4n)$  reaction. These bands have been interpreted as signature partners arising from

the coupling of the  $6_{5/2}$  proton intruder orbital with a  $^{190}\text{Hg}$  core. The two bands not only exhibit striking similarities with those observed in the other odd Tl isotopes with  $A = 193, 195$ , but also fit nicely in the systematics of all SD bands near  $A = 190$ . It is likely that it will be difficult to search for SD bands in even lighter Tl isotopes with detection systems similar to those used here. Such experiments will require the newer detector arrays with larger number of detectors.

## ACKNOWLEDGMENTS

This work has been sponsored by the Department of Energy, Nuclear Physics Division under contracts Nos. DE-FG05-87ER40361 (University of Tennessee), W-31-109-ENG-38 (Argonne) and DE-AC05-84OR21400 (Oak Ridge) and by the National Sciences and Engineering Research Council of Canada.

- 
- [1] E.F. Moore *et al.*, Phys. Rev. Lett. **63**, 360 (1989).
  - [2] R.V.F. Janssens and T.L. Khoo, Annu. Rev. Nucl. Part. Sci. **41**, 321 (1991), and references therein.
  - [3] M.A. Riley *et al.*, Nucl. Phys. **A512**, 178 (1990).
  - [4] E.F. Moore *et al.*, Phys. Rev. Lett. **64**, 3127 (1990).
  - [5] T. Lauritsen *et al.*, Phys. Lett. B **279**, 239 (1992).
  - [6] Y. Liang *et al.*, Phys. Rev. C **46**, R2136 (1992).
  - [7] R.R. Chasman, Phys. Lett. B **219**, 227 (1989).
  - [8] J. Becker, N. Roy, E.A. Henry, M.A. Deleplaque, C.W. Beausang, R.M. Diamond, J.E. Draper, F.S. Stephens, J.A. Cizewski, and M.J. Brinkman, Phys. Rev. C **41**, R9 (1990).
  - [9] D. Ye *et al.*, Phys. Rev. C **41**, R13 (1990).
  - [10] The term high-N intruder orbitals refers to orbitals located two major shells higher in energy in a spherical nucleus, which plunge down as a function of deformation and are near the Fermi surface for the SD shape.
  - [11] F.S. Stephens *et al.*, Phys. Rev. Lett. **65**, 301 (1990).
  - [12] F. Azaiez *et al.*, Phys. Rev. Lett. **66**, 1030 (1991).
  - [13] P.B. Fernandez *et al.*, Nucl. Phys. **A517**, 386 (1990).
  - [14] F. Azaiez *et al.*, Z. Phys. A **338**, 471 (1991).
  - [15] M.W. Drigert *et al.*, Nucl. Phys. **A515**, 466 (1990).
  - [16] J.M. Lewis (private communication).
  - [17] G. Palameta and J.C. Waddington, Nucl. Instrum. Methods A **234** 476 (1985).
  - [18] T. Lauritsen *et al.*, Phys. Rev. Lett. **69** 2479 (1992); T.L. Khoo *et al.*, Nucl. Phys. **A520**, 169c (1990).
  - [19] J.K. Johansson *et al.*, Phys. Rev. Lett. **63**, 2200 (1989).
  - [20] I.G. Bearden *et al.*, Report No. AECL 10613, 1992 (unpublished).
  - [21] W. Nazarewicz, J. Dudek, R. Bengtsson, T. Bengtsson, and I. Ragnarsson, Nucl. Phys. **A435**, 397 (1985).
  - [22] J. Dudek, Z. Szymanski, and T. Werner, Phys. Rev. C **23**, 920 (1981).
  - [23] M.W. Drigert *et al.*, Nucl. Phys. **A530**, 452 (1991).
  - [24] W. Satula, S. Cwiok, W. Nazarewicz, R. Wyss, and A. Johnson, Nucl. Phys. **A529**, 289 (1991).
  - [25] R. Bengtsson, S. Frauendorf, and F.R. May, At. Data Nucl. Data Tables **35**, 15 (1986), and references therein.
  - [26] T. Byrski *et al.*, Phys. Rev. Lett. **64**, 1650 (1990).
  - [27] F.S. Stephens, Nucl. Phys. **A520**, 91c (1990).
  - [28] I. Ahmad, M.P. Carpenter, R.R. Chasman, R.V.F. Janssens, and T.L. Khoo, Phys. Rev. C **44**, 1204 (1991).
  - [29] J.-Y. Zhang, R.F. Casten, W.-T. Chou, D.S. Brenner, N.V. Zamfir, and P. von Brentano, Phys. Rev. Lett. **69**, 1160 (1992).
  - [30] C. Baktash, J.D. Garrett, D.F. Winchell, and A. Smith, Phys. Rev. Lett. **69**, 1500 (1992).
  - [31] J.-Y. Zhang and L.L. Riedinger, Phys. Rev. Lett. **69**, 3438 (1992).
  - [32] R.V.F. Janssens *et al.*, Nucl. Phys. **A520**, 75c (1990).
  - [33] E.A. Henry (private communication).
  - [34] S.J. Krieger, P. Bonche, M.S. Weiss, J. Meyer, H. Flo-card, and P.H. Heenen, Nucl. Phys. **A542**, 43 (1992).